Adsorption and diffusion of H and O on an Ni(1 1 1) surface containing different amounts of Cr

doi: 10.1016/j.apsusc.2018.03.134

Contents lists available at ScienceDirect

Applied Surface Science

journal homepage: www.elsevier.com

Full Length Article

Adsorption and diffusion of H and O on an Ni(1 1 1) surface containing different amounts of Cr

Nishith Kumar Das*, Tetsuo Shoji

Frontier Research Initiative, New Industry Creation Hatchery Center, Tohoku University, 6-6-10 Aoba Aramaki, Aoba-ku, Sendai 980-8579, Japan

ARTICLE INFO

Article history:
Received 4 January 2018
Received in revised form 22 February 2018
Accepted 18 March 2018
Available online xxx

Keywords:
Oxidation initiation
Cr effects
O, H migration
DFT

ABSTRACT

Density functional theory (DFT) is used to calculate the adsorption and diffusion of atomic hydrogen and oxygen on Ni(1 1 1) and Ni—Cr(1 1 1) surfaces. The calculated results show that the adsorption energy (E_{ad}) of H and O gradually decreases when increasing their coverage of the surface, but the rate is very slow for H. H in the interstitial site significantly modifies the geometrical structure of the surface, and as a result, the metal–metal bond length is elongated. At high H coverage, the Ni—Cr bond length is noticeably elongated by interstitial H, indicating that Cr atoms are preferentially moved outward. Additionally, the activation energy of H is increased by Cr. Doping of Cr modifies the surface electronic structures, which can increase the energy barrier. For O, E_{ad} increases with increasing Cr content on top of the surface. The highest energy is attained by the surface with the most Cr on top. Metallic atoms are less mobile from the Ni or Cr rich region, and the mobility is high in less concentrated regions, especially at high O coverage. The activation energy of O is 0.41 eV for the path III, i.e., over the Ni—Cr bridge, which is 0.26 eV less than that of the pristine Ni(1 1 1) surface. The overall activation energy of O is increased on the Ni—Cr(1 1 1) surface compared to the pristine Ni(1 1 1) surface, which is consistent with experimental results. This study suggests that Cr atoms pulled away from the surface by H results in a cation vacancy on the surface. The process can accelerate surface oxidation at a very early stage. In contrast, Cr can trap atomic O and reduces its surface diffusivity, resulting in the formation of passive film in the Cr-rich region.

1. Introduction

Nickel-based alloys are widely used for advanced high-temperature structural components due to their good corrosion resistance and high strength in air and steam [1–4]. However, water vapor is present in nearly all atmospheres where nickel-based alloys are used. In the oxidation of metals, knowledge of the surface behavior of H and O is important because these atoms are frequently a product of oxidation reactions.

Extensive theoretical and experimental studies have been performed on nickel and nickel-based alloys to understand the oxide film property and its formation mechanism [5–15]. An experimental study on Ni—Cr alloy has suggested that the initial preferential oxidation of Cr is followed by a surface enrichment and oxidation of the remaining elements with lower affinity than oxygen [7]. The high mobility of chromium is attributed to the high preferential oxidation of Cr ions [16]. Additionally, the required amount of chromium improves corrosion properties and a chromium content of less than 10 wt.% is ineffective for forming a stable oxide film [5,6]. An atomic rearrangement in the thin film occurs due to oxygen exposure. Finally, a metal atom is segregated to the surface and becomes oxidized [17]. The presence of O and H on the surface accelerates the degradation of chromia forming alloys [18–21].

Additionally, most *ab initio* or molecular dynamics studies concerning corrosion have been restricted to atomic and molecular oxygen and hydrogen and water adsorption, dissociation and diffusion on Ni surfaces and bulk systems [11–14,22]. Those studies provide a fundamental understanding of adsorption, diffusion and metal atom segregation processes on the surface. Different stepped surface interactions with O and H have also been extensively studied [23,24]. In contrast, a limited number of studies have been carried out on oxygen, OH and water adsorption, dissociation and diffusion in Ni—Cr alloy surfaces using density functional theory (DFT) and quantum chemical molecular dynamics (QCMD) method [11,22]. DFT has shown that doping of Cr on the top layer nickel surface is beneficial for trapping atomic oxygen but it could preferentially dissolute from the surface to adsorb oxygen [11], which is in good agreement with experiment. Kim *et. al.* studied the interstitial diffusion of oxygen in a Ni—Cr binary alloy [25]. They found that the activation energy of oxygen diffusion in a Ni—Cr binary alloy is lower than that in pure nickel bulk, and it seems that the result tends to contradict the experimental data. The study suggests that oxygen diffuses more easily into the chromium matrix than into the nickel matrix because chromium

* Corresponding author.
Email addresses: nishith@fri.niche.tohoku.ac.jp (N.K. Das); tshoji@fri.niche.tohoku.ac.jp (T. Shoji)

https://doi.org/10.1016/j.apsusc.2018.03.134
0169-4332/

has a smaller atomic radius than nickel. Several binary or ternary alloy systems have been studied to predict the oxidation, surface ordering and segregation tendency of alloying elements using DFT [26–29]. Ti segregation is observed from surfaces upon adsorption of an oxygen atom [29]. For instance, Nolan et al. showed successive O_2 adsorption on the NiTi(110) surface, and they highlighted the oxygen adsorption induced formation of the TiO_x layer [30]. Mo atoms also have a segregation tendency for Ni-Mo(1 1 1) and Ni-Mo(100) surfaces [31], suggesting that the alloying element segregated from the surface in the presence of atomic oxygen leads to the formation of oxide film.

Chromium is one of the key alloying elements for forming protective chromium rich oxides on the surface of nickel-based alloys. Hydrogen and oxygen in alloys should affect the oxide formation process. Recent theoretical results have shown that doping of Cr increases the oxygen adsorption energies and the top layer metal atoms show outward relaxation due to an adsorbed oxygen on Ni(1 1 1) and Cr-doped Ni(1 1 1) surfaces [11]. Oxygen and hydrogen adsorption and diffusion on pristine nickel has been extensively studied but no theoretical studies have clarified the effect of Cr on atomic oxygen and hydrogen adsorption and diffusion on the surface. We, therefore, aim to clarify the interaction between O, H and the pristine Ni(1 1 1) and Ni—Cr(1 1 1) binary alloy surfaces using first-principles calculations. Different amounts of Cr are doped on top of the surface and subsurface and their interaction with different coverages of O and H is studied.

2. Computational details

First-principles calculations are carried out within the framework of the DFT as implemented in the Vienna *ab initio* simulation packages VASP [32,33]. The spin-polarized calculations are performed within the projector augmented wave (PAW) method [34]. We adopt the generalized gradient approximation (GGA) with the Perdew and Wang (PW91) functional for the exchange-correlation interaction [35]. The wave functions are expanded in terms of plane waves with in energy cutoff of 400 eV. The number of Monkhorst–Pack *k*-points is determined by performing individual DFT calculations on a nickel bulk and surface with an increasing number of *k*-points. An appropriate number of *k*-points is deemed to have been reached when a total energy convergence of 1 meV per atom is observed, and as a result a $16\times16\times16$ *k*-point is used for bulk Ni and $5\times5\times1$ *k*-point grid is used for the Ni(1 1 1) surface. The surface is described using a repeated slab approach. The Ni(1 1 1) surface consists of seven layers with a (2×2) supercell. A single H or O corresponds to 0.25ML coverage. The Cr-doped Ni system is modeled by replacing the Ni atoms on top, subsurface (second layer) and sub-subsurface (third layer) of the surface with Cr atoms. One, two and four Cr atoms are doped on the top of surface layer, hereafter, we call Ni-t1Cr (1 1 1), Ni-t2Cr(1 1 1) and Ni-t4Cr(1 1 1) surface, respectively, unless or otherwise states. We are also doped one and four Cr atoms on the subsurface and one Cr atom on the sub-subsurface, which we call Ni-2nd1Cr(1 1 1), Ni-2nd4Cr(1 1 1) and Ni-3rd1Cr(1 1 1), respectively. Fig. 1 shows model surfaces. Doping of Cr on top of nickel surface segregation is thermodynamically more stable than that of the subsurface. The DFT calculated segregation energy is 0.175 eV, which is in agreement with the results of Ruban [28]. One chromium atom doped into the subsurface and sub-subsurface layer exhibits the moderate segregation. The vacuum spacing is approximately 12 Å to ensure that there are no significant interactions between the slabs. The convergence tests for the Ni(1 1 1) surface indicates that this setup converge with respect to the slab thickness, vacuum spacing and *k*-point sampling. The energy relaxation iterates until the forces acting on all of the atoms are less than 10^{-3} eV/Å, with a convergence in the total energy about 10^{-5} eV. During the optimizations of the substrate structures, the first three layers from the bottom of the slab are fixed, whereas the other layers are fully relaxed to their lowest energy configurations with respect to all of the remaining degrees of freedom. The fixed layers are set to their bulk bond distances according to their optimized lattice constants which are determined from the bulk calculations.

Additionally, five layers slab with a (3×3) supercell is included in the reported results only where explicitly indicated. A $3\times3\times1$ k-point grid is used for (3×3) supercell and one, two and four Ni atoms on top of the surface are replaced with Cr atoms. Two different surfaces are modeled for the two and four Cr atoms containing surface, namely, Cr atoms sit in the first nearest neighbor (1NN) and second nearest neighbor (2NN) sites, as shown in Fig. S1. The convergence parameters, i.e., vacuum spacing, forces and energy, remain same as the (2×2) supercell. A single H or O corresponds to 0.11 ML coverage.

The lattice parameters for the Ni and Ni-3.125 at.%Cr have been obtained by fitting the calculated total energy with respect to the cell volume. The equilibrium lattice constant is 3.5175 Å for the Ni and 3.5178 Å for the Cr-doped Ni (3.125 at.% of Cr) bulk. The experimental lattice constant of nickel is 3.524 Å [36] and theoretically calculated lattice constant of Ni-Cr (3.125 at.% of Cr) is 3.52 Å [37], which is in good agreement with this study.

O and H are placed either directly on top positions (top site), between two metal atomic bonds as a bridge site, placed at the center of a hollow site in the second layer of atoms, directly below (hcp site), or at the center of a hollow site in the third layer of atoms directly below (fcc sites). H is also placed in interstitial octahedral and tetrahedral sites. The adsorption energy, E_{ad}, is calculated from the following formula:

$$E_{ad} = \left[E_{surf} + nE(O/H) - E_{system}\right]/n \quad (1)$$

where, E_{system} is the total energy of the adsorbate-surface system, E_{surf} is the energy of the surface, E (O/H) is the energy of the isolated atoms and n is the number of atoms. 15 Å cubic cell is used to calculate the atomic O and H energies.

Finally, the climbing image nudged elastic band (CI-NEB) method used to calculate the activation energy barriers (E_a) and the detailed reaction coordinates for the different steps [38].

3. Results and discussion

3.1. Revisited H adsorption on surface and subsurface sites

3.1.1. H Interaction with the Ni(1 1 1) surface

The E_{ad} is calculated with the variation of H coverage on Ni (1 1 1) and Ni—Cr (1 1 1) surfaces, as shown in Table 1. The calculated energy is 2.84 eV at 0.25 ML coverage. The experimental results suggest that the E_{ad} is in the range of 2.60–2.80 eV/atom [39,40] and the theoretical value vary from 2.89–2.95 eV/atom [41–46], which is consistent with this study. The E_{ad} of a (3×3) supercell is 2.85 eV, indicating that a slight increase of E_{ad} decreases the coverage to 0.11 ML. For a (2×2) surface, the energy is slightly increased with increasing coverage from 0.25ML to 0.50 ML. The behavior is different from that of other surfaces, but it is in good agreement with the previous study [42]. However, Table 1 shows that further increase of

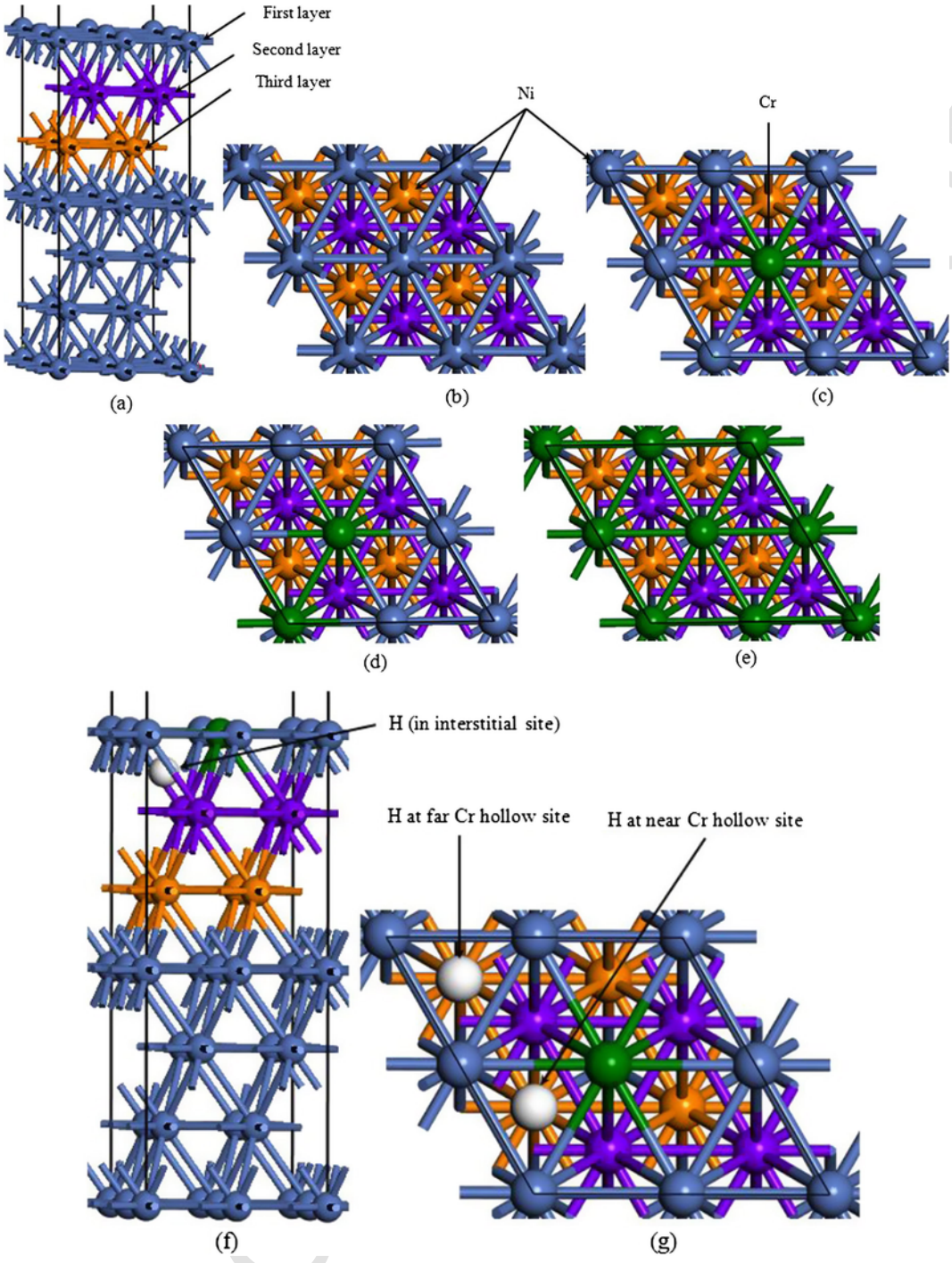

Fig. 1. (a) side and (b) top view of Ni(1 1 1) surface (c) Ni-t1Cr(1 1 1) surface (d) Ni-t2Cr(1 1 1) surface (e) Ni- t4Cr(1 1 1) surface (f) Ni-t1Cr(1 1 1) surface with H in the interstitial site and (g) Ni-t1Cr(1 1 1) surface with H on the surface.

coverage decreases the energy to 2.83 eV per atom. The most stable configurations show that H locates on the fcc hollow site, except for 0.50 ML coverage. In this case, one H on the fcc and another on the hcp site is the most stable configuration, whereas two H on the fcc site is approximately 40 meV less stable, as shown in Table 1. The calculated result is in excellent agreement with the result obtained by Greeley et al. [42,45]. We find that the E_{ad} of H decreases with increasing H coverage but the effect is not so significant. However, the calculated result is well consistent with the previous DFT study [45], though the value is slightly different. The previous study uses different atomic layer and surface size, which might explain this small energy difference.

The adsorption energy in the subsurface site is 2.20 eV, which is smaller than that of the surface sites. Ferrin et al. found that H in its preferred subsurface state is always less stable than its preferred surface state [44]. The H atom prefers to occupy the octahedral interstitial site. Table 1 shows that the adsorption energy is slightly increased with increasing coverage in the interstitial site. This result suggests

Table 1
The calculated H adsorption energies on Ni(1 1 1) and Ni—Cr(1 1 1) surfaces. Letters in parenthesis shows H position.'f' means fcc site, 'h' means hcp site, 'f1' means far Cr fcc site, 'f2' means near Cr fcc site and 'h1' means far Cr hcp site.

No. of H	H position	Ni (1 1 1)		Ni-t1Cr(1 1 1)		Ni-2nd1Cr(1 1 1)		Ni-3rd1Cr(1 1 1)	
1H	On surf.	2.84 (f)	2.83 (h)	2.95 (f1)	2.94 (f2)	2.89 (h)	2.87 (f2)	2.89 (f1)	2.87 (h)
	Subsurf.	2.20		2.24		2.23		2.26	
2H	On surf.	2.88 (f+h)	2.84 (f)	2.98 (f1+h1)	2.94 (h+f2)	2.87 (h+f2)	2.86 (f2)	2.88 (f1)	2.87 (f2+h)
	Subsurf.	2.23		2.25		2.22		2.27	
3H	On surf.	2.83 (f)	2.82 (h)	2.88 (2f2+f1)	2.86 (f2)	2.86 (f2)	2.83 (h)	2.87 (f1)	2.86 (f2+f1)
	Subsurf.	2.25		2.28		2.23		2.29	
4H	On surf.	2.83 (f)	2.82 (h)	2.85 (3f2+f1)	2.83 (3h+h1)	2.82 (3f2+f1)	2.81 (3h+h1)	2.86 (f)	2.85 (h)
	Subsurf.	2.28		2.28		2.25		2.31	

that accumulating H in the subsurface region does not have any effect on E_{ad}. In fact, the metal-hydrogen binding becomes slightly stronger. H gradually increases strain in the structure, which might increase the metal-hydrogen binding energy. A previous study showed that increasing the lattice strain increased the adsorption energy [42].

The Ni-H bond length is 1.70 Å at 0.25 ML. This calculated value is consistent with the theoretical result [45] but marginally shorter than the experimentally observed value [47]. The Ni—H bond length is shortened with increasing H on the surface. The distance between the first and second layer metallic atoms increases to adsorb H. The Ni—Ni bond length between the first and second layer is increased by 0.02 Å for an H atom on the fcc site, which is consistent with the value observed of Bhatia et al. [48]. Increasing coverage on the surface gradually increases the metallic bond lengths, e.g., the average bond extension is approximately 1.0% at 0.25 and 0.50 ML, and then it is increased by 1.8% and 2.3% at 0.75 and 1.0 ML coverage, respectively. It is experimentally observed that adsorption of H at 185 K to a coverage of 0.73 ML generates an outward relaxation of 1.3 ± 0.4% by the surface atoms [49]. In contrast, H in the interstitial site noticeably increases the distance between two layers. Increasing the number of interstitial H increases the bond distance. The nearest Ni—Ni bond length is elongated by 1.9% at 0.25 ML coverage and the highest bond extension is 7.0% by accommodating four H in the interstitial site. It is very likely that the nearest bond elongation occurs at low coverage, whereas, at high coverage, the bond distance increases uniformly. Low-energy electron diffraction (LEED) studies reported that the metal-metal bond expansion varies from 2.5% to 4.6% due to H atoms occupying interstitial sites [50,51]. Hydrogen in metal elongates the local metallic bonds resulting in a weaker host bond strength [46,52,53]. The increasing H content in the subsurface region produces localized strain on the surface that might increase E_{ad} but alleviate the mechanical property of materials.

3.1.2. H Interaction with the Ni—Cr(1 1 1) surface

H at the far Cr fcc site is the most stable with the E_{ad} 2.95 eV, as shown in Table 1. The E_{ad} of H on the Ni-t1Cr (1 1 1) surface increases approximately 110 meV at 0.25 ML coverage compared to the pristine Ni (1 1 1) surface. Two fcc, i.e., the near Cr and far Cr sites, are energetically very competitive for adsorbing H. H at the far Cr fcc site is only 10 meV more stable than H at the near Cr fcc site, and the hcp site is the third most stable position with an E_{ad} of 2.90 eV. The E_{ad} of H for the Ni-t1Cr(1 1 1) (3 × 3) surface is shown in Table 1S. The Ni(1 1 1) (3 × 3) surface containing one Cr shows that the E_{ad} of H at the near Cr and far Cr 2NN fcc site is 2.95 eV and 2.90 eV, respectively. This result is in good agreement with the previous DFT study [22]. Additionally, the hcp near Cr and hcp far Cr sites are 50 meV and 70 meV less stable than the most stable fcc hollow site for the (3 × 3) surface, respectively. H moves far from Cr, decreasing the E_{ad} and the value remains close to that of the pristine Ni(1 1 1) surface. However, the E_{ad} increases from 2.95 eV to 2.98 eV per atom with increasing coverage from 0.25 ML to 0.50 ML, and then the energy gradually decreases with increasing coverage. The trend is very similar to that of the pristine Ni(1 1 1) surface, suggesting that H coverage has a small effect on the adsorption energy.

The energy and adsorption site are slightly changed to move the Cr atom from on top of the surface to the subsurface. Table 1 shows that the energy slightly decreases when Cr locates at the subsurface and sub-subsurface layers. Notably, H shows higher energy at the hcp site than the fcc site, although the latter surface is only 20 meV less preferable. Cr at the sub-subsurface containing surface slightly increases the E_{ad} compared to the pristine Ni(1 1 1) surface at 0.25 ML coverage and fcc far Cr site is the most stable position. H in the interstitial site shows a slight increase of E_{ad} with increasing coverage, which is the same result as that obtained on the pristine Ni(1 1 1) surface.

The Ni—H bond distance varies from 1.68 Å to 1.70 Å and the Cr—H bond distance varies from 1.80–1.82 Å, as shown in Table 4. The short Ni—H bond reveals that H makes a preferable bond with Ni rather than Cr. The change of metallic bond length for the most stable systems is shown in Table 2. The Ni—Ni bond length is usually elongated and the Ni—Cr bond distance is elongated or contracted depending on the location of H. For the Ni-t1Cr(1 1 1) surface, the Ni—Ni bond length is elongated by 1.0% and the Ni—Cr bond length is contracted by 0.4% to adsorb a single H on the surface. Further addition of H on the surface increases the expansion and contraction process. The highest expansion and contraction is observed at 1.0 ML. The Ni—Ni and Ni—Cr bond distances are changed by 3.7% (expansion) and 7.0% (contraction), respectively. H in the interstitial site elongates Ni—Ni and Ni—Cr bond lengths. A remarkable structural damage occurs by accommodating four H

Table 2
The metallic bond length elongation (%) of Ni—Cr(1 1 1) surfaces.

Surface	H position	Bond	1H	2H	3H	4H
Ni-t1Cr(1 1 1)	On surface	Ni—Ni	1.0	2.0	3.0	3.7
		Ni—Cr	−0.4	−1.5	−5.0	−7.0
	Subsurface	Ni—Ni	2.0	2.4–3.7	5.7	7.3
		Ni—Cr	3.0	5.0	6.5	9.5
Ni-2nd1Cr(1 1 1)	On surface	Ni—Ni	0.4	1.0	2.0	2.0
		Ni—Cr	1.6	3.0	2.0	3.7
	Subsurface	Ni—Ni	2.0	4.0	5.6	7.0
		Ni—Cr	4.0	5.3	6.1	9.8
Ni-3rd1Cr(1 1 1)	On surface	Ni—Ni	1.0	1.0	2.0	3.0
		Ni—Cr	0.0	0.0	0.0	0.0
	Subsurface	Ni—Ni	1.2	2.0	4.8	6.4
		Ni—Cr	0.4	−0.6	−0.6	−1.0

'-' Means contraction.

atoms in interstitial sites. The Ni—Ni and Ni—Cr bond elongations are approximately 7.3% and 9.5%, respectively. With Cr in the subsurface, the Ni—Cr bond length slightly increases for a single H on the surface. However, Cr in the sub-subsurface region does not change the Ni—Cr bond length at any coverage, which is expected because adsorbed H might have less interaction with the third layer metallic atom [45]. However, the expansion and contraction of the Ni—Cr bond length can modify the surface geometry. This unequal bond elongation makes the surface uneven and produces strain in the structure, which leads to a decrease of the host bond strength. This result cannot be directly compared with any experimental observation but the phenomenological behavior can be observed. The corrosion behavior and the microstructure of the oxide film are affected by H dissolved in the nickel-based alloy [54]. Additionally, H in the alloy also results in a thicker, defective inner layer and a discontinuous outer layer of the oxide, in conjunction with the depletion of Cr. Our results suggest that Cr is preferentially moved outward due to the presence of H in the interstitial site. This preferential movement might cause the depletion of Cr from the surface during high temperature oxidation.

3.1.3. Activation energy of H on the Ni(1 1 1) and Ni—Cr(1 1 1) surfaces

The calculated E_a of H is shown in Fig. 2. For the pristine Ni (1 1 1) surface, the most preferable diffusion path is fcc-bridge-hcp (path I) with an E_a of 0.25 eV and fcc-top-hcp (path II) is least preferable. This is in good agreement with previous experimental and theoretical results [55–57]. However, the calculated E_a of H on the Ni(1 1 1) surface is 70 meV larger than the experimental value [55], possibly due to the temperature, coverage and computational parameters. Previous DFT studies obtained noticeably smaller values of 0.15 eV and 0.135 eV [48,56,57]. The differences in the computational parameters between this study and Refs. [57,58], such as exchange-correlation functional, lattice constant, surface size, and k-points are noted. For example, Kristinsdóttir et al. obtained an E_a of 0.15 eV [57], where the bulk Ni lattice constant is 3.56 Å. In addition, the slab surface consisted of three layers where the top layer is allowed to relax. Increasing the lattice constant seemingly generates strain on the surface, which reduces the energy barrier [42]. The number of layers affects the inward and outward interlayer relaxations, as demonstrated in experimentally [58,59]. A DFT study showed that these surface changes can affect the energy barrier [56].

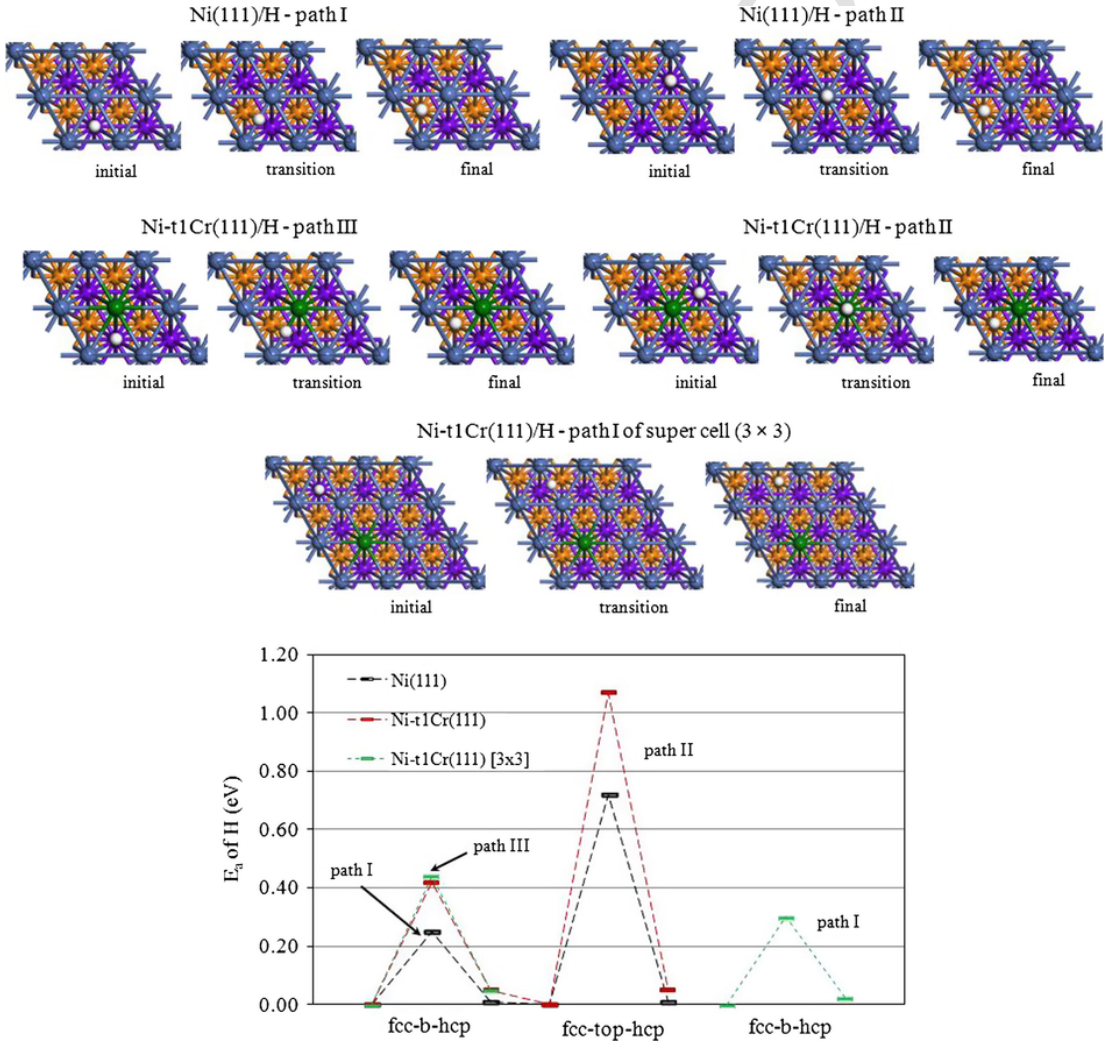

Fig. 2. Activation energy of H on Ni(1 1 1) and Ni-t1Cr(1 1 1) surfaces.

Moreover, the vacuum thickness of less than 10 Å might also affects on the value, which uses in the previous study [48]. The energy barrier of H is 0.92 eV for diffusing from the surface fcc site to the subsurface octahedral site. The value is 40 meV and 80 meV larger than previous theoretical results [45] and 80 meV lower than the temperature programmed desorption (TPD) result [60]. Considering the zero-point energy (ZPE) correction reduces the value to 0.90 eV, which is excellent agreement with the value obtained by Greeley et al. [45]. The remaining small deviation might be due to different slab sizes and optimization parameters. Hence, the calculated E_a of H on the Ni(1 1 1) surface is reasonable.

Doping of Cr remarkably increases the E_a of H at the near Cr sites, as shown in Fig. 2 and Table 2S. However, Cr does not modify the diffusion path. The energy barriers are less affected by Cr while H diffuses between two hollow sites at the second nearest neighbor (2NN) Cr sites. For instance, the energy barrier reduces to 0.29 eV for path I. To fully understand the Cr effect, several calculations have been performed on a (3 × 3) supercell containing one Cr on top of the surface. The E_a is 0.44 eV for the fcc-bridge-hcp (path III), i.e., over the Ni—Cr bridge. The (3 × 3) supercell is 20 meV higher in energy compared to the (2 × 2) supercell for the same path. The pristine Ni (3 × 3) supercell is also overestimated 20 meV of E_a for H compared to the (2 × 2) supercell. The size and layer difference might be the reason for this discrepancy. However, this behavior reveals that Cr increases the energy barrier. The energy barrier decreases to 0.30 eV and 0.32 eV for the fcc (2NN)-bridge-hcp (2NN) and hcp (2NN)-bridge-fcc paths, respectively.

The diffusion of H from surface to subsurface is considered near the Cr site. The E_{ad} of H is almost unchanged when Cr locates at the 2NN or far site. Thus, it is reasonable to consider H diffusivity through the near Cr site only. The energy barrier is 1.24 eV without the ZPE correction, which is 0.32 eV larger than that of the pristine Ni(1 1 1) surface, indicating that the presence of Cr can slow the diffusivity of H from the surface to subsurface. Several experimental studies confirmed that the activation energy of H is higher in alloy 690 than alloy 600 and Ni bulk [61]. Alloy 690 has high Cr and low Ni. Additionally, the 5 at.% of Cr in iron is almost double the E_a of H compared to iron [62]. The electrochemical permeation method has also demonstrated the increase of the E_a of H in the presence of Cr in α-iron [62]. Those studies suggested that the energy barrier of H is increased by the presence of Cr in the lattice although the materials and conditions are different from this study. However, our calculated result suggests that Cr on top of the Ni(1 1 1) surface can increase the activation energy of H. This observation is well consistent with the available literature [61,62]. Cr is unlikely to form a bond with H and modify surface electronic interactions that may influence the energy barrier.

3.1.4. Electronic interaction

Bader charge analysis performed to explain the adsorption energy and local geometry. The calculated atomic charges are shown in Table 3. One can see that H receives more electrons on the surface than the subsurface and increasing coverage gradually decreases the amount of charge of H. For the Ni—Cr(1 1 1) surface, the charge transfer from the metal atom to H is increased compared to the pristine Ni(1 1 1) surface, e.g., one H receives approximately 0.31 *e* from the Ni(1 1 1) surface, whereas, it receives 0.37 *e* from the Ni—Cr(1 1 1) surface. H located far from Cr receives less charges from the surface. It is no wonder that H receives electrons from the metal atoms and becomes negatively charged [22,53]. However, the most interesting feature is that doping of Cr on the surface increases charge transfer to H, but this extra amount of charge is not donated by Cr.

Table 3
Bader charge analysis.

Surfaces	Ni – 1st	Ni – 2nd	Cr	H
Ni (1 1 1)	−0.02	+0.02		
Ni—Cr (1 1 1)	−0.25	−0.02	+0.86	
Ni (1 1 1) – H on surf.	0.10			−0.31
Ni (1 1 1) – H oct.	0.05			−0.28
Ni (1 1 1) – 4H surf.	0.29			−0.28
Ni (1 1 1) – 4H oct.	0.17	0.07		−0.25
Ni—Cr(1 1 1) – H on surf.	0.12		0.10	−0.37
Ni—Cr(1 1 1) – H oct.	0.05		0.05	−0.32
Ni—Cr (1 1 1) – 4H on surf.	0.39		0.33	−0.33
Ni—Cr (1 1 1) – 4H oct.	0.13	0.13	0.11	−0.27

More importantly, the nearest Ni atom donates a substantially larger amount of charge to the H than the Cr atoms and this interaction modifies the local electronic structure. This result suggests that Ni prefers to bind with H whereas Cr does not, which might be a reason for the increase of the activation energy. Additionally, the process leads to Ni atoms being more positively charged, and as a result, strong repulsion occurs with the positively charged Cr. This repulsive interaction helps to move the Cr atom away from the surface, followed by elongation of the Ni—Cr bond length.

3.2. O Adsorption with the variation of surface coverage

3.2.1. O On the Ni(1 1 1) surface

Number of studies have been performed on O adsorption on Ni (1 1 1) and Ni—Cr (1 1 1) surfaces [11,15,23,63,64]. Those studies have confirmed that the fcc hollow site is the most stable site for O adsorption. The calculated E_{ad} for the most stable fcc site is 5.44 eV, and the hcp site is only 0.10 eV less stable, which is in good agreement with previous studies [11,15]. Decreasing the coverage of O to 0.11 ML increases E_{ad} by 5.49 eV for the fcc site, as shown in Table 3S.

For high coverage, O atoms are placed on the surface in different combinations, such as all fcc, all hcp, or a combination of fcc and hcp and a combination with top and bridge sites, although those sites are not preferable for adsorbing an atomic O. Increasing the coverage gradually decreases the adsorption energy, as shown in Fig. 3 and Table 4S. Strong adosorbate-adsorbate interactions are revealed by theoretical and experimental observations [23,65–67]. For 0.5 ML coverage, the most stable structure can accommodate two O atoms on the fcc hollow site followed by two O atoms on the hcp as the second most stable structure. The latter structure is 0.11 eV lower in energy than that of former surface. The E_{ad} and position of O is in excellent

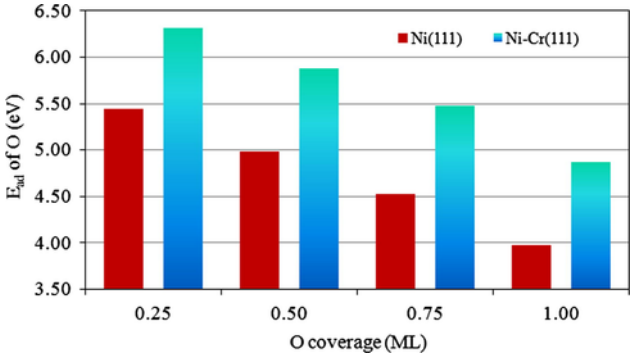

Fig. 3. Adsorption energy of O on Ni(1 1 1) and Ni-t1Cr(1 1 1) surfaces with the variation of coverage.

agreement with the previous theoretical study [23]. An oxygen molecule is placed on the surface with different orientations. The adsorption energy is 1.93 eV and 1.92 eV per molecule for the top-hcp-bridge (t-h-b) and top-fcc-bridge (t-f-b) orientation, respectively, suggesting that adsorption of atomic O on the surface is much more preferential than molecular adsorption, but molecular adsorption can also occur. The calculated bond length of O_2 is 1.45 Å. Molecular adsorption of O_2 on the Ni (1 1 1) surface was also previously studied by theoretical and experimental methods [68–70]. The most preferable site is the top-hcp-bridge with a parallel orientation [68,69] and the bond length of O_2 is 1.46 Å [69]. The E_{ad} on the hollow site with the perpendicular orientation is 1.07 eV per molecule and the bond length is 1.31 Å. O_2 on the Ni(1 1 1) surface can be adsorbed in either a parallel or perpendicular orientation but the parallel orientation is obviously preferable.

Three O atoms are absorbed on fcc sites at 0.75 ML coverage. The second most stable structure retains O on the hcp sites, and the E_{ad} is 0.12 eV per atom less than that of the most stable configuration. The E_{ad} is decreased to 3.95 eV per atom at 1.0 ML coverage. Both hollow sites, i.e., fcc and hcp, are equally preferable. O atoms are placed at different positions with different combinations, but the final structure results in O on the fcc or hcp sites. In case of molecular adsorption, two O molecules are placed on surface in parallel and perpendicular orientation. The calculated structure shows that O molecules can be adsorbed in a parallel or perpendicular orientation. The absorption energy is 1.52 eV per molecule for the parallel orientation. The bond length of O_2 is 1.377 Å, indicating that the bond is elongated versus the gas phase. This result suggests that O_2 can be adsorbed on the Ni (1 1 1) surface at high coverage.

The metal-oxygen bond distances are shown in Table 6. The Ni—O bond distance varies from 1.81 Å to 1.84 Å. The bond length is slightly smaller at high coverage than at low coverage. A previous near-edge X-ray absorption fine structure (NEXAFS) [71] and DFT result for the Ni—O bond length is 1.85 Å [11] and a LEED result is 1.83 Å [72]. The top layer metal atoms show outward movement to adsorb O on the surface [11,73]. The nearest Ni—Ni bond length is increased by 3.0% and the bond length far from O is extended by 1.0% at 0.25 ML. With increasing coverage the average metallic bond length increases, i.e., the bond length between the first and second layer extends approximately 3.0% at 1.0 ML and the length between the second and third layer also increases approximately 1.0%. This is because all fcc sites are occupied by O and the metal-oxygen interaction uniformly pulls the top layer metallic atoms.

3.2.2. O on the Ni—Cr (1 1 1) surface

Atomic O prefers the fcc hollow near Cr site of the Ni—Cr(1 1 1) surface [11,74]. This study also finds that the fcc hollow near Cr site is the most stable site. Moreover, the fcc hollow far Cr site is 0.90 eV less stable than the most stable site, suggesting a strong interaction between O and Cr. The (2 × 2) supercell is too small to fully study the interaction between Cr and O. The large (3 × 3) supercell result is shown in Table 5S. Table 5S shows that the E_{ad} of O on the fcc site is 6.35 eV, 5.62 eV and 5.55 eV for the nearest, second nearest and third nearest position, respectively, which reveals that O binding with the surface is affected by Cr. However, moving Cr into a subsurface layer has almost no effect on O adsorption, e.g., the energy is 5.51 eV and 5.49 eV for the most stable configuration for Cr at the subsurface and sub-subsurface, respectively. We, therefore, focus on the top of the Cr-doped Ni(1 1 1) surfaces.

The E_{ad} is 6.31 eV at 0.25 ML and decreases by 5.88 eV per atom at 0.5 ML coverage, as shown in Table 6S. For the latter case, two competitive structures are found. The most stable structure adsorbs O atoms in two ways; first, both O locate at the fcc near Cr site and second, two O atoms are at the fcc and hcp near Cr sites. When both O atoms are placed on the hcp hollow near Cr site, the E_{ad} is approximately 0.06 eV less than that of the most stable site. The E_{ad} decreases by 5.40 eV per atom for a structure with one O at the near Cr fcc and one O at the far Cr fcc. This energy value clearly suggests that Cr has a strong influence on the O adsorption process. When an O_2 is placed on the Ni-t1Cr(1 1 1) surface in different orientations, it seems that the adsorption process is different from that of the pristine Ni(1 1 1) surface. The energy is 2.58 eV per molecule and 2.56 eV per molecule for the t-f-b and t-h-b sites, respectively, and the bond length of O_2 is 1.486 Å and 1.474 Å, respectively. The adsorption site changes to move O_2 upward and consequently, the energy and bond length are slightly reduced. For instance, the t-b-t and f-t-h sites have an energy of 2.37 eV/mole and 2.29 eV/mole, respectively.

The most stable structure at 0.75 ML coverage accommodates three O at the near Cr fcc or hcp site. The E_{ad} for the second most stable structure is 5.16 eV per atom with two O at the near Cr site and one O at the far Cr site. The E_{ad} is further decreased by 5.01 eV per atom for the structure that contains one O near Cr and two O atoms at the far Cr sites. For 1.0 ML, four O atoms occupy the fcc site in the most stable structure. Different structures are optimized, e.g., the initial structure contains three O atoms at the near Cr fcc and one O at the near Cr hcp site but the final structure has four O atoms at the fcc hollow site, which confirms that O at the fcc hollow site is the most stable structure. At the same coverage, two O_2 were placed on the surface, and the optimized structure shows that the two O_2 are almost perpendicularly adsorbed near the Cr fcc site with an E_{ad} of 1.39 eV per molecule and an O_2 bond length of approximately 1.32 Å.

The average bond length of Cr—O is 1.75 (±0.02) Å and the Ni—O bond distance is approximately 1.87 Å for the Ni-t1Cr(1 1 1) surface. The calculated bond lengths are in good agreement with the previous study [11]. The shorter Cr—O bond length indicates their preferential interaction. The top layer nickel atoms move slightly upward to adsorb O at different coverages [11]. The most notable structural change is observed at 1.0 ML coverage. Up to 0.75 ML, the Ni—Cr bond length is increased by 0.5–1.5% and the Ni—Ni bond length is increased by 2.0–3.5%. Adding one more O to the surface, which represents 1.0 ML coverage, significantly changes the surface structure. The Ni—Cr and Ni—Ni bond distances are elongated by 14.0% and 1.0%, respectively, and as a result Cr pulls out from its initial position. Additionally, when Cr starts moving upward, Ni atoms show less movement from the surface. The process helps Ni to remain on the surface and possibly form an Ni-rich inner oxide layer. Recent experimental studies have shown that Cr is enriched with O on Ni—Cr alloy surfaces at room temperature [8,16,54], indicating a high mobility for Cr in the Ni lattice [16]. The atomic scale result is in excellent agreement with experimental observation [7,54]. Cr has a high affinity to O which attributes to the Cr movement, especially at high coverage. A recent in-situ TEM study found that the addition of Cr at.5.0% to Ni increases the rate of vacancy injection compared with pure Ni [16]. The preferential upward movement of Cr from the surface with high coverage of O, whereas the pristine nickel surface does not show such behavior, could be occurring at the early stage of oxidation at very low temperature, resulting in cation vacancies on the surface.

3.2.3. Activation energy of oxygen

Several theoretical and experimental studies show that the activation energy of O varies from 0.54 eV to 0.64 eV on Ni surfaces [75,76]. Our calculated energies are shown in Fig. 4. The E_a is 0.67 eV for path I. The value is 80 meV larger than the previous DFT result and interestingly is very close to the experimental result. In-

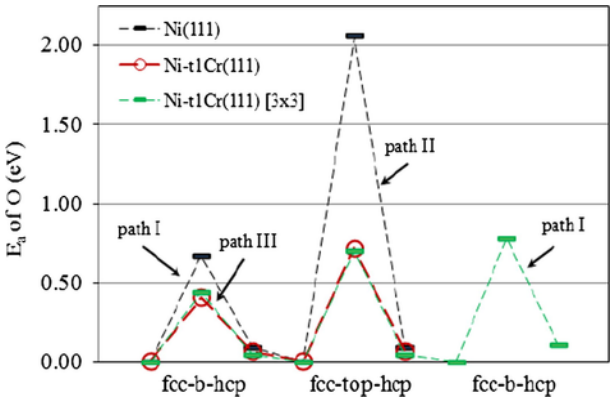

Fig. 4. Activation energy of O on Ni(1 1 1) and Nit1Cr(1 1 1) surfaces.

creasing the surface size from the (2 × 2) to (3 × 3) supercell decreases the surface coverage from 0.25 ML to 0.11 ML. The latter surface gives an energy barrier of 0.65 eV, which is close to the (2 × 2) surface and experimental result as well. Diffusion through path II has a very high energy barrier of 2.06 eV.

The presence of Cr on top of the surface noticeably modifies the energy barrier. The energy barrier is reduced to 0.41 eV for path III, which is 0.26 eV less than that of the pristine Ni(1 1 1) surface. Kim et al. also showed by DFT that Cr in bulk Ni decreases the energy barrier approximately 0.41 eV [25]. Thus, the phenomenon is well consistent with the previous study. The large surface, i.e., (3 × 3) supercell obtains an E_a of 0.45 eV for path III. The (3 × 3) supercell has a higher Ni concentration than that of the (2 × 2) supercell. Increasing the Ni concentration at the nearest sites could reasonably increase the size of this small energy barrier. Path II, i.e., hcp-top-fcc is less preferable but the E_a is significantly lower than that of the pristine Ni(1 1 1) surface. For the far Cr site, the E_a is 0.78 eV for the hcp(2NN)-bridge-fcc(2NN) site for the (3 × 3) supercell, which is 0.13 eV higher than that of the pristine Ni(1 1 1) surface, indicating that Cr slightly decreases the diffusivity of O on the surface. The local electronic structure is modified by Cr, which could be a reason for the change in the size of this small energy barrier.

3.3. The effect of Cr concentration on O and H adsorption and diffusion

3.3.1. H adsorption properties

The calculated E_{ad} of H on different surfaces is listed in Table 4. The energy is increased with increasing Cr concentration on top of the surface and the highest value is attained by the Ni-t4Cr (1 1 1) surface. In contrast, the Ni-2nd4Cr (1 1 1) surface has the lowest E_{ad} of H, and consequently, subsurface Cr weakens the Ni—H bond strength. When the Cr concentration is very low at the subsurface the effect is not obvious. We attribute the result to a modification of the local electronic structure in the subsurface that might affect the adsorption process. The Cr containing surface reduces the energy 0.17 eV per H atom with increasing H coverage from 0.25 ML to 1.0 ML, whereas the pristine Ni(1 1 1) surface has almost no effect. H coverage is also less pronounced for the surface containing Cr at the subsurface region. This reveals that Cr does influence H adsorption phenomenon and the effect is smaller for the pristine Ni(1 1 1) surface. H in interstitial sites has a lower energy than H on the surface and more importantly, increasing H coverage slightly increases the E_{ad}, which is similar to the results for the Ni(1 1 1) surface.

The Ni—H bond distance varies from 1.67 Å to 1.70 Å and the Cr—H bond length varies from 1.80 Å to 1.84 Å. The shortest Cr—H bond length is 1.80 Å for the Ni-t4Cr (1 1 1) surface with 0.75 and 1.0 ML coverage. The Ni—H bond length is always smaller than the Cr—H bond length to make a preferential bond between Ni and H rather than Cr and H. It is well known that an adsorbent can elongate the distance between the first two layers and the elongation is heightened to increase the coverage of adsorbent. The calculated values are shown in Table 5. For the Ni-t2Cr (1 1 1) surface with one H, the Ni—Cr bond length decreases approximately 0.8% and Cr moves slightly away from H along the x- and y-axis. Ni atoms move 0.01 Å toward H along the y-axis and the Ni-Ni bond length increases approximately 2.0%. Increasing H on the surface further decreases the Ni—Cr bond length and increases the Ni—Ni bond length. It is interesting to find that H on the surface has less effect on the Ni—Cr bond length of the Ni-t4Cr(1 1 1) surface. The H atom shows less preference to bond with the Cr, which might attribute to the result. This phenomenon is consistent for the Ni-2nd4Cr(1 1 1) surface because Cr atoms are situated in the subsurface region and have a negligible interaction with H, and Ni on top of the surface moves toward the H atom resulting in outward relaxation. H in the interstitial site increases the bond length, and the effect is more detrimental when Cr content is high. This phenomenon indicates that Cr steps away from H and Ni moves toward H, resulting in an uneven surface or a metallic vacancy generates on the surface. This structural modification can accelerate surface oxidation at a very early stage.

Table 4
The E_{ad} (eV) and metal-H bond distances (Å) on different Ni—Cr(1 1 1) surfaces.

Surface	H position	1H	2H	3H	4H	Ni—H	Cr—H
Ni(1 1 1)	On surface	2.84 (2.85)	2.88	2.83	2.83	1.68–1.70	
	Interstitial	2.20	2.23	2.25	2.28		
Ni-t2Cr(1 1 1)	On surface	3.11 (2.98)	3.16	3.08	2.95	1.67–1.70	1.80–1.
	Interstitial	2.22	2.23	2.24	2.26		
Ni-t4Cr(1 1 1)	On surface	3.21 (3.05)	3.19	3.09	3.04		1.80–1.
	Interstitial	2.15	2.17	2.19	2.18		
Ni-2nd4Cr(1 1 1)	On surface	2.67	2.71	2.67	2.68	1.68–1.72	
	Interstitial	2.09	2.11	2.15	2.18		

Note – The value in parenthesis corresponds to (3 × 3) supercell.

Table 5
The average metallic bond elongation (%).

Surface	H position	Bond	1H	2H	3H	4H
Ni-t2Cr(1 1 1)	On surface	Ni—Ni	2.0	2.8	4.0	7.3
		Ni—Cr	−0.8	−1.5	−3.0	−7.8
	Subsurface	Ni—Ni	3.0	5.0	6.5	7.9
		Ni—Cr	2.3	4.0	5.8	9.2
Ni-t4Cr(1 1 1)	On surface	Ni—Ni				
		Ni—Cr	<0.4	<0.3	<0.2	<0.2
	Subsurface	Ni—Ni				
		Ni—Cr	3.5	5.7	7.7	10.0
Ni-2nd4Cr(1 1 1)	On surface	Ni—Ni				
		Ni—Cr	1.2	2.4	2.4	3.7
	Subsurface	Ni—Ni				
		Ni—Cr	2.0	4.8	7.7	9.5

'-' Means contraction.

3.3.2. O adsorption properties

Oxygen behaves very different than H. The calculated properties are shown in Table 6. A strong interaction between Cr and O is observed and such an interaction increases their binding energy [76], which is very likely to increase the E_{ad} of O with increasing Cr concentration on the top layer of the surface. The energy decreases when moving the Cr into the subsurface and sub-subsurface layers. The Ni-t4Cr (1 1 1) surface, which is fully covered by Cr, has the highest E_{ad} of 7.46 eV at 0.25 ML. The fcc hollow site becomes the second most stable site. Usually, the fcc hollow site is most stable for O adsorption but the highly Cr containing surface is changed the most favorable adsorption site from fcc to hcp. The behavior remains consistent throughout the coverage of O from 0.25 ML to 1.0 ML. The geometrical structure is very similar for the fcc and hcp site adsorbed surfaces. For example, the Cr—O bond distance and the movement of Cr are almost unchanged. The electronic contribution from the hcp adsorbed surface is 0.1 *e* higher than that of the fcc adsorbed surface, perhaps explaining this discrepancy.

To further understand the effect of Cr concentration on O adsorption, we performed calculations on different Cr containing (3 × 3) supercells, as shown in Table 7. It is possible to vary the distance between two Cr atoms on the large supercell. Localized Cr clearly shows a strong binding with O. Decreasing Cr locally also decreases the E_{ad} of O. For instance, two Cr at the 1NN site show a strong binding with O compared to two Cr at the 2NN site. The calculated energy is 6.45 eV for the latter surface, which is almost same value as that of the 1NN Cr containing surface with O at the near one Cr hollow site. This is because O can directly interact with only one Cr and the second Cr atom locates at the 2NN site that has less interaction with the adsorbent, thus the adsorption process becomes weak. This observation is also consistent with the results of other Cr containing Ni(1 1 1) surfaces. The highest E_{ad} of 7.50 eV is attained by the surface with three Cr at the nearest site. The same energy value is obtained by two different surfaces, i.e., three Cr surrounded fcc and hcp sites. Four Cr at the nearest site is 0.15 eV less stable than the most stable surface and the fcc site is 0.04 eV more preferable than the hcp site, which is not consistent with the (2 × 2) surface. A higher percentage of Cr may change the adsorption site. The four Cr containing surface should have the highest energy of O but this is not the case here, because the three Cr containing Ni(1 1 1) surface donates approximately 1.39 *e* and the four Cr containing Ni(1 1 1) surface donates approximately 1.28 *e* to the nearest O and Ni atoms. Additionally, the Cr—O bond distance is 1.87 Å for the former surface, whereas the distance is 1.88 Å for the latter case, indicating a negative effect by the fourth Cr that increases the Cr—O bond distance. The process reveals a slightly weak interaction that might reduce this small amount of energy. However, the lowest energy is attained by the three Ni surrounded sites even when the surface has a high Cr content. As a whole, localized Cr shows a strong binding with O, which is in support of the passivation initiation process. An experimental study on nickel-based alloys observed that a layer of Cr-rich film is very quickly formed on alloy surfaces [78]. An X-ray photoelectron spectroscopy (XPS) study found that Cr can selectively be oxidized on the surface [79]. A theoretical study also showed a preferential bonding form between Cr and O [77]. This reveals that the more protective continuous film can be formed on the alloy surface that contains high chromium.

The repulsive interaction between O—O is very likely at high coverage, which diminishes the energy [66,67]. Notably, the Cr containing surface always has higher energy than that of the pristine Ni(1 1 1) surface. At 1.0 ML coverage, the E_{ad} of O is increased approximately forty and seventy percent for Ni-t2Cr(1 1 1) and Ni-t4Cr(1 1 1) surfaces compared to Ni(1 1 1) surface, respectively, whereas Cr in the subsurface layer slightly decreases the energy. The rate of energy decrease is slow at the high Cr containing surface compared to pristine Ni(1 1 1) or low Cr containing surfaces, as shown in Fig. 5. Localized Cr can successfully trap more O atoms nearby, which might initiate passive film formation.

The Cr—O and Ni—O distances varied from 1.78 Å to 1.86 Å and from 1.82 Å to 1.86 Å, respectively. Increasing O coverage increases the bond distance between Cr and O. The metallic bond length is also extended due to the presence of O on the surface. We

Table 6
The E_{ad} (eV) and bond distances (Å) on different Ni—Cr(1 1 1) surfaces.

Surface		1O	2O	3O	4O	Ni—O	Cr—O
Ni(1 1 1)	fcc	5.44	4.99	4.53	3.98	1.81–1.84	
Ni-t2Cr(1 1 1)	fcc	7.10 (7.04)	6.63	6.08	5.56	1.85–1.86	1.78–1.84
	hcp	7.26	6.69; 6.73 [1f+1 h]	6.09	5.54	1.84–1.86	1.77–1.84
Ni-t4Cr(1 1 1)	fcc	7.23 (7.19)	7.04	6.76	6.50		1.78–1.86
	hcp	7.46	7.22	6.96	6.68		1.78–1.86
Ni-2nd4Cr(1 1 1)	fcc	5.28	4.75	4.25	3.71	1.82–1.85	
	hcp	5.38	4.77	4.16	3.66		

Note – The value in parenthesis corresponds to (3 × 3) supercell.

Table 7
The E_{ad} of O on different Cr containing Ni(1 1 1) surfaces.

Surfaces	O Position	Near 3Cr	Near 2Cr	Near 1Cr	Near 3Ni
Ni—Cr(1 1 1) – 1Cr	fcc			6.35	5.55
	hcp			6.30	5.45
Ni—Cr(1 1 1) – 2 Cr (1NN)	fcc		7.04	6.40, 6.33	5.60
	hcp		7.02	6.44, 6.30	5.43
Ni—Cr(1 1 1) – 2 Cr (2NN)	fcc			6.45	5.60
	hcp			6.38	5.46
Ni—Cr(1 1 1) – 4 Cr (3Cr-1NN)	fcc	7.50	6.88	6.30	5.64
	hcp		6.97	6.21	5.43
Ni—Cr(1 1 1) – 4 Cr (4Cr-1NN)	fcc	7.35	6.64	6.11, 5.98	5.55
	hcp	7.31	6.65	6.19, 6.01	5.48

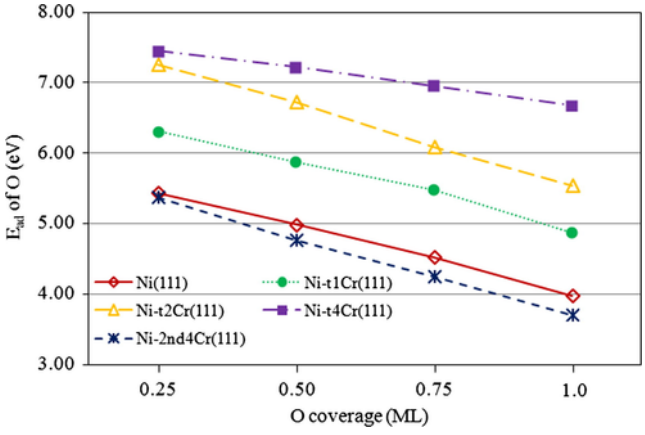

Fig. 5. Adsorption energy of O on different surfaces with the variation of O coverage.

measured the metallic bond lengths of the most stable structure, found that the Ni—Cr bond extension varies from 0.5% to 3.6% and the Ni—Ni bond extension varies from1.0% to 3.0% with varying coverage of O from 0.25 ML to 1.0 ML for the Ni-t2Cr(1 1 1) surface. The bond extension varies from 1.0% to 2.5% for the Ni-t4Cr(1 1 1) surface. Additionally, Cr also moves laterally and the displacement is approximately 0.06 Å along the x- or y-axis for the Ni-t2Cr(1 1 1) surface. The extension is more pronounced when Cr is present at the subsurface layer. Less mobility of metallic atoms is observed at the locally Cr rich or Ni rich region and the mobility is high when the nearest neighbors are heterogeneous species, especially at high coverage of O.

3.3.3. Activation energies of atomic H and O

The Cr on top of the surface plays a significant role in the adsorption process. It would be interesting to see how Cr concentration effects the energy barrier of O and H. The calculated activation energies are shown in Fig. 6. The E_a of H on the Ni-t2Cr(1 1 1) surface is 0.36 eV for hcp-bridge-fcc (path IV), i.e., over the Cr—Cr bridge, and the barrier is 0.41 eV for path III. For the (3 × 3) supercell, the energy barriers are 0.44 eV and 0.42 eV for path IV and path III of the Ni(1 1 1) surface containing two Cr, respectively. The E_a is decreased to 0.37 eV for path I. The highest activation energy is found near Cr sites. However, the energy barrier is lowest over the Ni—Ni bridge and the value increases with increasing Cr content. Cr atoms on the surface can modify the surface geometry and electronic structure nearby, which can decrease the diffusivity of H on the surface. It is experimentally observed that the energy barrier of H is higher in alloy 690 compared to alloy 600 [61]. The experimental studies considered the bulk system and our calculations consider the surface. The calculated value should therefore be different from experimental results. However, a qualitative agreement between our study and the experimental result is seen. The metal-H bond distance shows that H prefers to bond with Ni and avoids Cr. Moreover, Cr can increase the electron transfer from the surface to H and the donation from Ni atoms rather than Cr is increased. These factors might dominate the diffusion of H on the surface.

The E_a of O is 0.45 eV for path IV of Ni-t2Cr(1 1 1) and 0.43 eV for the (3 × 3) supercell. Further increase of Cr content increases E_a to 0.55 eV and 0.52 eV for the (2 × 2) and (3 × 3) supercells, respectively. For high Cr surfaces, the Cr atom is moved along the x- and y-axis for fcc and hcp sites during the adsorption of O. This lateral movement is not uniform for O at fcc and hcp sites and these metal atom displacements are considered in the model for the activation energy calculation, resulting in an increased E_a. The phenomenon is identical for the (2 × 2) and (3 × 3) supercells. The effect of cell size and Cr concentration causes a small energy difference between the two systems. Moreover, the diffusivity of O is analyzed for path I and E_a is 0.78 eV, which is same as the value obtained for the Ni(1 1 1) surface containing one Cr. The value is further increased to 0.85 eV for the same path for the Ni(1 1 1) surface containing four Cr. Increasing Cr can modify the surface electronic structure, which increases the energy barrier. This study suggests that the overall diffusivity of O is decreased on the Ni—Cr(1 1 1) surface compared to the pristine Ni(1 1 1) surface, which is qualitatively in agreement with the experimental observation [80]. Increasing Cr content on the surface reduces the diffusivity of O, resulting in the formation of a protective film in the Cr—rich region and thus an increase of the material's resistivity.

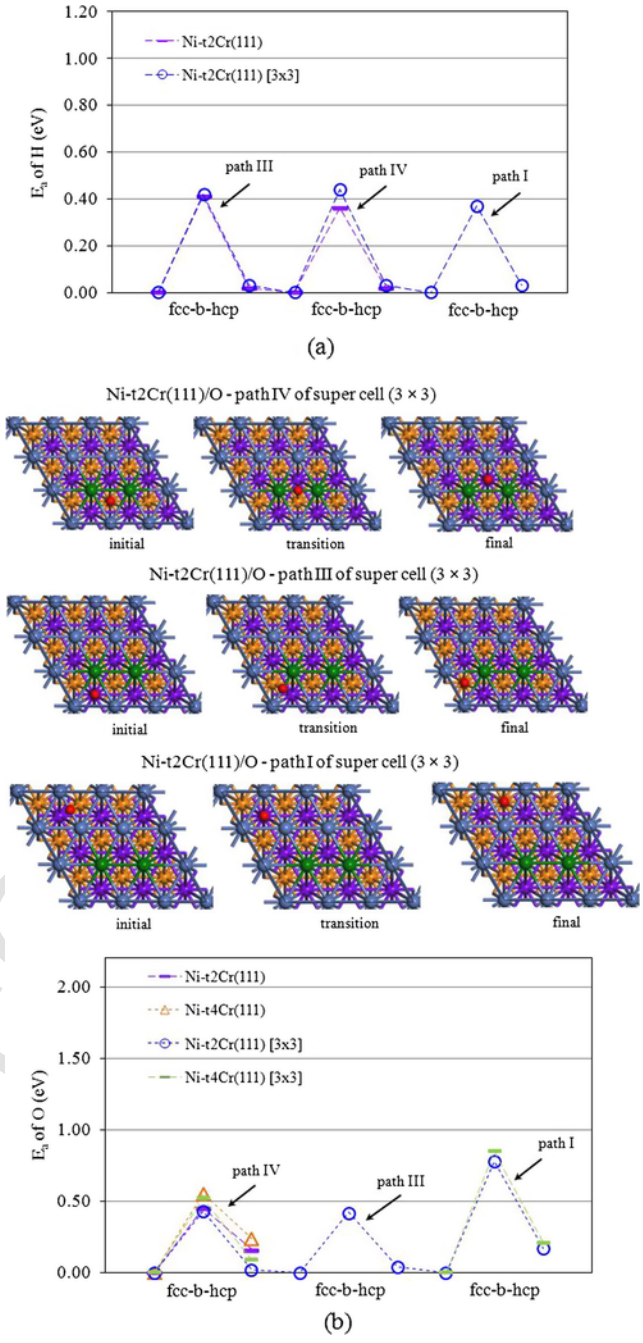

Fig. 6. Activation energy of (a) H and (b) O on different Cr containing Ni(1 1 1) surfaces.

4. Conclusions

DFT results show that the E_{ad} of H and O gradually decreases with increasing coverage on the surface, but for H, the effect is not so significant. The E_{ad} of H in the subsurface site is smaller than that of the surface sites and H prefers to stay at the octahedral interstitial site. Increasing H coverage in the interstitial site slightly increases E_{ad}, which is the opposite result of surface adsorption phenomena. H on Ni—Cr (1 1 1) increases the energy with increasing Cr content,

and the overall energy trend remains identical to that of the pristine Ni(1 1 1) surface.

Increasing H coverage on the surface extends the Ni—Ni bond length and contracts the Ni—Cr bond length. The average bond extension is 2.3% at 1.0 ML coverage for the Ni(1 1 1) surface, whereas at 1ML coverage on the Ni—Cr(1 1 1) surface, the Ni—Ni bond expansion is approximately 3.7% and Ni—Cr bond contraction is approximately 7.0%. Increasing Cr decreases the effect of H on geometrical evolution. However, the structural damage is more significant for H in the interstitial site. At 1.0 ML, the Ni—Ni bond elongation is 7.0% for Ni(1 1 1), and the elongation is 7.3% for Ni—Ni and 9.5% for Ni—Cr for Ni—Cr(1 1 1) surfaces, which reveals that Cr is preferentially moved outward by interstitial H.

The E_a of H in Ni(1 1 1) is 0.25 eV for path I, i.e., hcp-bridge-fcc and 0.92 eV for the surface to the first subsurface diffusion, which is an excellent agreement with the theoretical result. The value is increased to 0.44 eV for path III, i.e., over the Ni—Cr bridge and 1.24 eV for surface to subsurface diffusion for the Ni-t1Cr(1 1 1) surface. Bader charge analysis reveals that doping of Cr increases charge transfer to H, but this extra amount of charge is donated by Ni atoms. Ni prefers to bind with H, whereas Cr does not.

The E_{ad} of O is higher for the Ni—Cr(1 1 1) surface than the pristine Ni(1 1 1) surface. An atomic O located near the Cr hollow site is the most stable configuration, and moving to the far Cr site notably diminishes the energy. Increasing coverage gradually decreases the adsorption energy to obtain a strong adsorbate-adsorbate interaction. The highest E_{ad} is attained by the surface with three Cr at the nearest site or with full Cr covered. The nearest metal-metal bond length is increased by O. However, the Ni—Cr bond length is noticeably elongated at 1 ML for the Ni-t1Cr(1 1 1) surface but this remarkable structural damage is not observed for Ni-t2Cr(1 1 1) and Ni-t4Cr(1 1 1) surfaces.

The energy barrier of O is 0.41 eV for path III, i.e., over the Ni—Cr bridge, which is 0.26 eV less than that of the pristine Ni(1 1 1) surface. Increasing Cr content not only slightly increases the E_a of O at the near Cr site but also the far Cr site. We find that E_a of O for path IV, i.e., over Cr—Cr bridge, is 0.45 eV and 0.52 for Ni-t2Cr(1 1 1) and Ni-t4Cr(1 1 1) surfaces, respectively. For the (3×3) supercell, the energy barrier is 0.78 eV and 0.85 eV over the Ni—Ni bridge for two and four Cr containing Ni(1 1 1) surfaces, respectively. Increasing Cr modifies the surface electronic structure, leading to an increase of the energy barrier. The overall diffusivity of O is therefore slow on the Ni—Cr(1 1 1) surface compared to the pristine Ni(1 1 1) surface, which is in good agreement with experimental results.

Acknowledgements

DFT calculation has been performed by supercomputing resources. The authors gratefully acknowledge SR11000 supercomputing resources from the Center for Computational Materials Science of the Institute for Materials Research, Tohoku University. We also would like express our sincere thanks to the crew of this center.

Appendix A. Supplementary material

Supplementary data associated with this article can be found, in the online version, at https://doi.org/10.1016/j.apsusc.2018.03.134.

References

[1] W.E. Ruther, S. Greenberg, J. Electrochem. Soc. 111 (1964) 1116–1121.
[2] G.R. Holcomb, J. Electrochem. Soc. 156 (2009) C292–C297.
[3] I.G. Wright, R.B. Dooley, Int. Mater. Rev. 55 (2010) 129–167.
[4] H. Buscail, R. Rolland, C. Issartel, F. Rabaste, F. Riffard, L. Aranda, M. Vilasi, J. Mater. Sci. 46 (2011) 5903–5915.
[5] N. Birks, H. Rickert, J. Inst. Metals 91 (1963) 308.
[6] C. Giggins, F. Pettit, Trans. Met. Soc. AIME 245 (1969) 2495–2507.
[7] J. Steffen, S. Hofmann, Surf. Interf. Anal. 11 (1988) 617–626.
[8] G.B. Hoflund, W.S. Epling, Chem. Mater. 10 (1998) 50–58.
[9] A.A. Ul-Hamid, Anti-Corros. Methods Mater. 51 (2004) 216–222.
[10] L. Luo, L. Zou, D.K. Schreiber, M.J. Olszta, D.R. Baer, S.M. Bruemmer, G. Zhou, C.M. Wang, Chem. Commun. 52 (2016) 3300–3303.
[11] N. K. Das, T. Shoji, Appl. Surf Sci 258 (2011) 442-447 Corros. Sci. 73 (2013) 18–31.
[12] O. Assowe, O. Politano, V. Vignal, P. Arnoux, B. Diawara, O. Verners, A.C.T. van Duin, J. Phys. Chem. A 116 (2012) (1805) 11796–11801.
[13] C. Taylor, R.G. Kelly, M. Neurock, J. Electrochem. Soc. 153 (2006) E207–E214.
[14] G.C. Wang, S.X. Tao, X.H. Bu, J. Catal. 244 (2006) 10–16.
[15] N. Cherbal, E.H. Megchiche, H. Zenia, K. Lounis, M. Amarouche, Appl. Surf. Sci. 663 (2017) 62–70.
[16] C.-M. Wang, A. Genc, H. Cheng, L. Pullan, D.R. Baer, S.M. Bruemmer, Sci. Rep. 4 (2014) 3683.
[17] R. Hsiao, D. Mauri, Appl. Surf. Sci. 157 (2000) 185–190.
[18] B. Tveten, G. Hultquist, T. Norby, Oxid. Met. 52 (1999) 221–233.
[19] Q. Yang, J.G. Yu, J.L. Luo, J. Electrochem. Soc. 150 (2003) B389–B395.
[20] D. Wallinder, G. Hultquist, B. Tveten, E. Hörnlund, Corros. Sci. 43 (2001) 1267–1281.
[21] J. Yuan, W. Wang, H. Zhang, L. Zhu, S. Zhu, Corros. Sci. 109 (2016) 36–42.
[22] N.K. Das, T. Shoji, Int. J. Hydrogen Energy 38 (2013) 1644–1656.
[23] T. Li, B. Bhatia, D.S. Sholl, J. Chem. Phys. 121 (2004) 10241–10249.
[24] R.A. Olsen, S.C. Bădescu, S.C. Ying, E.J. Baerends, J. Chem. Phys. 120 (2004) (1863) 11852–11861.
[25] J.J. Kim, S.H. Shin, J.A. Jung, K.J. Choi, J.H. Kim, Appl. Phys. Lett. 100 (2012) 131904.
[26] K.J. Andersson, F. Calle-Vallejo, J. Rossmeisl, I. Chorkendorff, J. Am. Chem. Soc. 131 (2009) 2404–2407.
[27] C.A. Menning, J.G. Chen, J. Chem. Phys. 130 (2009) 174709.
[28] A. Ruban, H. Skriver, J.K. Nørskov, Phys. Rev. B 59 (1999) 15990–16000.
[29] M. Nolan, S.A.M. Tofail, Biomaterials 31 (2010) 3439–3448.
[30] M. Nolan, S.A.M. Tofail, Phys. Chem. Chem. Phys. 12 (2010) 9742–9750.
[31] A.U. Nilekar, A.V. Ruban, M. Mavrikakis, Surf. Sci. 603 (2009) 91–96.
[32] G. Kresse, J. Hafner, Phys. Rev. B 47 (1993) 558.
[33] G. Kresse, J. Furthmuller, Phys. Rev. 54 (1996) 11169–11186.
[34] G. Kresse, D. Joubert, Phys. Rev. 59 (1999) 1758.
[35] J.P. Perdew, Y. Wang, Phys. Rev. 45 (1992) 13244.
[36] J.R. Neighbours, F.W. Bratten, C.-S. Smith, J. Appl. Phys. 23 (1952) 389–393.
[37] D. Kim, S.-I. Shang, Z.-K. Liu, Comput. Mater. Sci. 47 (2009) 254–260.
[38] G. Mills, H. Jónsson, G.K. Schenter, Surf. Sci. 324 (1995) 305–337.
[39] K. Christmann, Z. Naturfosch. 34a (1979) 22–29.
[40] K. Christmann, R.J. Behm, G. Ertl, M.A. Van Hover, W.H. Weinberg, J. Chem. Phys. 70 (1979) 4168–4184.
[41] H. Yang, J.L. Whitten, J. Chem. Phys. 98 (1993) 5039–5049.
[42] J. Greeley, W.P. Krekelberg, M. Mavrikakis, Angew. Chem. Int. Ed. 43 (2004) 4296–4300.
[43] J. Greeley, M. Mavrikakis, J. Chem. Phys. 109 (2005) 3460–3471.
[44] P. Ferrin, S. Kandoi, A.U. Nilekar, M. Mavrikakis, Surf. Sci. 606 (2012) 679–689.
[45] J. Greeley, M. Mavrikakis, Surf. Sci. 540 (2003) 215–229.
[46] E. Shustorovich, R.C. Baetzold, Science 227 (1985) 876–881.
[47] L. Hammer, H. Landskron, W. Nichtl-Pecher, A. Fricke, K. Heinz, K. Müller, Phys. Rev. B 47 (1993) 15969.
[48] B. Bhatia, D.S. Sholl, J. Chem. Phys. 122 (2005) 204707.
[49] J.A. Davies, D.P. Jackson, P.R. Norton, Solid Stat. Commu. 34 (1980) 41.
[50] D. Lacina, J.L. Erskine, Phys. Rev. B 76 (2007) 104103.
[51] S.C. Jung, M.H. Kang, Phys. Rev. B 72 (2005) 205419.
[52] H. Adachi, S. Imoto, J. Phys. Soc. Japan 46 (1979) 1194–1200.
[53] Y. Itsumi, D.E. Ellis, J. Mater. Res. 11 (1996) 2206–2213.
[54] J. Hou, Q.J. Peng, K. Sakaguchi, Y. Takeda, J. Kuniya, T. Shoji, Corros. Sci. 52 (2010) 1098–1101.
[55] G.X. Cao, E. Nabighian, X.D. Zhu, Phys. Rev. Lett. 79 (1997) 3696–3699.
[56] G.W. Watson, R.P.K. Wells, D.J. Willock, G.J. Hutchings, J. Phys. Chem. B 105 (2001) 4889–4894.
[57] L. Kristinsdóttir, E. Skúlason, Surf. Sci. 606 (2012) 1400–1404.
[58] H. Lu, E. Gusev, E. Garfunkel, T. Gustafsson, Surf. Sci. 352–354 (1996) 21–24.
[59] H.B. Michaelson, J. Appl. Phys. 48 (1977) 4729–4733.
[60] K.J. Maynard, A.D. Johnson, S.P. Daley, S.T. Ceyer, Faraday Discuss. 91 (1991) 437–449.
[61] M. Uhlemann, B.G. Pound, Corros. Sci. 40 (1998) 645–662.
[62] H. Hagi, J. Japan Inst. Metals 55 (1991) 1283.

[63] W.-B. Zhang, C. Chuan, H.-Q. Xie, J. Phys. Soc. Japan 82 (2013) 074709.
[64] B. Hammer, L.B. Hansen, J.K. Nørskov, Phys. Rev. B 59 (1999) 7413–7421.
[65] C. Wu, D.J. Schmidt, C. Wolverton, W.F. Schneider, J. Catal. 286 (2012) 88–94.
[66] J.T. Stuckless, C.E. Wartnaby, N. Al-Sarraf, St.J.B. Dixon-Warrne, M. Kovar, D.A. King, J. Chem. Phys. 106 (1997) 2012–2030.
[67] S.D. Miller, N. Inoglu, J.R. Kitchin, J. Chem. Phys. 134 (2011) 104709.
[68] S. López-Moreno, A.H. Romero, J. Chem. Phys. 142 (2015) 154702.
[69] F. Mittendorfer, A. Eichler, J. Hafner, Surf. Sci. 433–435 (1999) 756–760.
[70] M. Beutl, K.D. Rendulic, G.R. Castro, Surf. Sci. 385 (1997) 97–106.
[71] M. Pedio, L. Becker, B. Hillert, S. D'Addato, J. Haase, Phys. Rev. B 41 (1990) 7462.
[72] D.T. Vu Grimsby, Y.K. Wu, K.A.R. Mitchell, Surf. Sci. 232 (1990) 51–55.
[73] T. Narusawa, W.M. Gibson, E. Törnqvist, Phys. Rev. Lett. 47 (1981) 417–420.
[74] N.K. Das, W.A. Saidi, J. Chem. Phys. 146 (2017) 154701.
[75] G. Binnig, H. Fuchs, E. Stoll, Surf. Sci. Lett. 169 (1986) L295–L300.
[76] H.O. Nam, I.S. Hwang, K.H. Lee, J.H. Kim, Corros. Sci. 75 (2013) 248–255.
[77] N.K. Das, T. Shoji, J. Phys. Chem. C 116 (2012) 13353.
[78] P. Combrade, P. M. Scott, M. Foucault, E. Andrieu, E. Marcus, Proceedings of the 12th International Conference on Environmental Degradation of Materials in Nuclear Power System – water reactors, Salt Lake City, Utah, 14 August – 18 August 2005, edited by T. R. Allen, P. J. King, and L. Nelson (TMS, USA, 2005).
[79] S.P. Jeng, P.H. Holloway, C.D. Batich, Surf Sci 227 (1990) 278–290.
[80] B. Chattopadhyay, G.C. Wood, Oxid. Met. 2 (1970) 373–399.